UDC: 519.63; 517.958
MSC 2020: 35K57, 35B40, 60J27, 65M08, 65M12
DOI: 10.5281/zenodo.19635808

On Global Solvability, Entropy Dissipation, and Numerical Analysis of Reaction-Diffusion Systems with Cross-Diffusion and Markov Kinetics

E. Yu. Shchetinin, A. A. Shevchuk

Abstract

This paper studies multicomponent reaction-diffusion systems with cross-diffusion and Markov kinetics in an entropy-structured setting. The topic is important because cross-diffusion models generally lack a universal maximum principle, may be nonsymmetric or degenerate, and therefore require methods beyond standard parabolic theory to prove solvability and quantify relaxation to equilibrium. The aim is to identify subclasses of such systems for which existence, entropy dissipation, uniqueness, regularity, and numerical behavior can be analyzed.

The object of study is a system of coupled diffusion-reaction equations in a bounded domain with no-flux boundary conditions, where the reaction operator is generated by a continuous-time Markov chain. The analysis combines entropy variables, the boundedness-by-entropy framework, logarithmic Sobolev inequalities in the spatial domain, a modified logarithmic Sobolev inequality for the finite-state chain, an energy-based weak-strong uniqueness argument, and interior regularity theory for diagonal uniformly parabolic systems. A key step is the exact decomposition of relative entropy into density and composition parts, which separates spatial and kinetic dissipation channels.

For the entropy-structured subclass satisfying the assumptions of the external boundedness-by-entropy theorem, weak entropy solutions are obtained globally in time. For a narrower diagonal uniformly parabolic subclass, weak-strong uniqueness and interior Hölder regularity are proved. In the conservative no-sink regime, exponential convergence to equilibrium is established for smooth positive solutions together with a lower bound for the relaxation rate. Numerical experiments for a three-component system on grids up to 256 by 256 show monotone decay of the discrete entropy. In the diagonal conservative test, the observed relaxation rates are 2.94 and 2.97 versus a theoretical reference value of 3.00, with relative errors of 2.0 and 1.0 percent; in the strongly coupled nondiagonal case, the observed rates are 2.85 and 2.60, showing qualitative agreement and the influence of stronger coupling. The results clarify relaxation mechanisms and support entropy-consistent numerical approximations.

Keywords: cross-diffusion, entropy variables, boundedness by entropy, Markov kinetics, modified logarithmic Sobolev inequality, entropy dissipation, weak-strong uniqueness, Hölder regularity, numerical experiments.

Funding: This work received no dedicated external funding.

1 Introduction

Reaction-diffusion systems with cross-diffusion arise in problems of multicomponent mass transport, mixture theory, population dynamics, chemical kinetics, and several models of mathematical biophysics. Their characteristic feature is that the flux of each component depends not only on its own gradient but also on the gradients of the other components. As a result, the diffusion matrix is typically nonsymmetric and need not be positive definite in the standard Euclidean sense. For this reason, no universal form of the maximum principle is available for such systems, and the analysis must rely on other structural arguments.

For a broad class of such systems, the entropy structure plays a central role. If there exists a strictly convex entropy H and a symmetric positive semidefinite mobility matrix B for which the factorization (6) holds, then after passing to the entropy variables

$$w = \nabla H(u) \tag{1}$$

the diffusion part takes a symmetrized form. This makes it possible to derive a priori entropy estimates and to build a theory of weak solutions even when the coefficients degenerate on the boundary of the admissible state set.

In a number of applications, the reaction part is naturally generated by a continuous-time Markov chain. Under detailed balance, the entropy dissipation of the reaction operator is expressed through the Dirichlet form associated with the chain generator. This leads to the use of modified logarithmic Sobolev inequalities and, in conservative regimes, to quantitative relaxation estimates.

The present work combines three lines of analysis. The first concerns global existence of weak entropy solutions in an entropy-structured class. The second concerns quantitative entropy dissipation and exponential convergence to equilibrium in a special conservative regime. The third covers weak-strong uniqueness and interior Hölder regularity in a narrower diagonal uniformly parabolic subclass.

Let us stress one methodological point from the outset. The paper does not formulate a new general existence theorem for an arbitrary class of cross-diffusion systems. The existence block relies on the external entropy framework of A. Jüngel [10]. The paper's own contribution consists of the following:

1) a class of systems with Markov kinetics is identified for which the hypotheses of the external existence theorem can be verified in terms of the assumptions used here;

2) an exact decomposition of the relative entropy into density and composition parts is obtained;

3) an explicit lower bound for the relaxation rate is derived,

$$\lambda_* = \min\{2\beta_* \lambda_{\mathrm{LSI}}(\Omega),\, \lambda_{\mathrm{MLSI}}(Q)\};$$

4) the computational section is presented as a reproducible numerical study consistent with the analytical part.

The main original analytical result is contained in Section 4. Its key feature is that the spatial and kinetic channels of entropy decay are controlled by different functional constants, namely $\lambda_{\mathrm{LSI}}(\Omega)$ and $\lambda_{\mathrm{MLSI}}(Q)$. For the class under consideration, this gives a transparent interpretation of the interaction between diffusion and Markov kinetics.

The paper is organized as follows. Section 2 states the model, the system of assumptions, and the definition of a weak entropy solution. Section 3 discusses the existence block as an application of an external entropy theorem and proves weak-strong uniqueness in the diagonal subclass. Section 4 is devoted to entropy dissipation and exponential relaxation. Section 5 deals with interior Hölder regularity. Section 6 presents numerical experiments. Section 7 states the limits of applicability of the results. Section 8 contains the conclusion.

2 Problem Setting and Assumptions

2.1 The system

Let $\Omega \subset \mathbb{R}^d$, $d \geq 1$, be a bounded connected domain, let $T > 0$, and set $Q_T = \Omega \times (0, T)$. We consider the system

$$\partial_t u - \nabla \cdot (A(u)\nabla u) = Qu - S(u) \quad \text{in } Q_T, \tag{2}$$

with the no-flux boundary condition

$$(A(u)\nabla u)\nu = 0 \quad \text{on } \partial\Omega \times (0, T), \tag{3}$$

and the initial data

$$u(\cdot, 0) = u^0 \quad \text{in } \Omega. \tag{4}$$

Here $u = (u_1, \dots, u_n)$ is the vector of unknown concentrations, $A(u) \in \mathbb{R}^{n\times n}$ is the diffusion matrix, $Q \in \mathbb{R}^{n\times n}$ is the generator of a continuous-time Markov chain, and $S(u)$ is a nonlinear sink term.

2.2 Map of assumptions

For logical clarity, the assumptions are divided into three blocks.

Block E (existence) is used in the proof of global weak entropy solutions.

Block D (dissipation) contains additional conditions needed for a quantitative estimate of entropy dissipation and exponential convergence to equilibrium.

Block R (regularity) contains additional assumptions used in the proof of weak-strong uniqueness and interior Hölder regularity.

This separation is essential: the results in these blocks apply to different and, in general, incomparable classes of models. In particular, weak-strong uniqueness and regularity are not an automatic continuation of the general existence block; they are proved only after a substantial restriction of the class.

2.3 Assumptions for existence

(E1) Geometry of the domain. The domain Ω is bounded, connected, and has Lipschitz boundary.

(E2) Separable entropy and entropy factorization. There exist an open convex set of admissible states $D \subset (0, \infty)^n$, a separable entropy

$$H(u) = \sum_{i=1}^{n} h_i(u_i), \tag{5}$$

where $h_i \in C^2((0, \infty))$ are strictly convex, and a matrix $B \in C^1(D; \mathbb{R}^{n\times n})$, symmetric and positive semidefinite, such that

$$A(u) = B(u)H''(u) \qquad \text{for all } u \in D. \tag{6}$$

Moreover, the mapping $\nabla H \colon D \to \mathbb{R}^n$ is a diffeomorphism onto its image.

(E3) Coercivity of the entropy. For every $C > 0$, the sublevel set $\{u \in D \colon H(u) \leq C\}$ is relatively compact in D.

(E4) Markov reaction. The matrix $Q = (q_{ij})$ is the generator of a continuous-time Markov chain:

$$q_{ij} \geq 0 \ (i \neq j), \qquad \sum_{i=1}^{n} q_{ij} = 0 \quad \text{for all } j. \tag{7}$$

The matrix Q is assumed to be irreducible.

(E5) Compatibility of the reaction-sink term with the entropy. There exists a constant $C_R > 0$ such that

$$\nabla H(u) \cdot (Qu - S(u)) \leq C_R(1 + H(u)) \qquad \text{for all } u \in D. \tag{8}$$

(E6) Invariance of the admissible set. It is assumed that the set D is positively invariant under the reaction-sink field

$$R(u) := Qu - S(u), \tag{9}$$

and that, within the existence theorem, this condition is understood as the assumption of positive invariance of the admissible set in the external entropy result being used.

(E7) Initial data.

$$u^0 \in L^1(\Omega; \mathbb{R}^n), \qquad u^0(x) \in D \text{ for a.e. } x, \qquad \int_\Omega H(u^0(x))\, \mathrm{d}x < \infty. \tag{10}$$

2.4 Additional assumptions for entropy dissipation

In Section 4 we consider the conservative case

$$S \equiv 0. \tag{11}$$

(D1) Logarithmic entropy.

$$H(u) = \sum_{i=1}^{n} (u_i \log u_i - u_i). \tag{12}$$

(D2) Detailed balance. There exists an invariant measure $\pi = (\pi_1, \ldots, \pi_n)$, $\pi_i > 0$, $\sum_i \pi_i = 1$, such that

$$\pi_i q_{ij} = \pi_j q_{ji} \qquad \text{for all } i, j. \tag{13}$$

(D3) Spatial logarithmic Sobolev inequality. The domain Ω satisfies an LSI with constant $\lambda_{\mathrm{LSI}}(\Omega) > 0$:

$$\int_\Omega f \log \frac{f}{\bar{f}}\, \mathrm{d}x \leq \frac{1}{2\lambda_{\mathrm{LSI}}(\Omega)} \int_\Omega \frac{|\nabla f|^2}{f}\, \mathrm{d}x \tag{14}$$

for all nonnegative f with $\bar{f} = |\Omega|^{-1} \int_\Omega f\, \mathrm{d}x$.

(D4) Modified logarithmic Sobolev inequality for the chain. There exists a constant $\lambda_{\mathrm{MLSI}}(Q) > 0$ such that for every density

$$f = (f_1, \ldots, f_n), \qquad f_i > 0, \qquad \sum_{i=1}^{n} \pi_i f_i = 1, \tag{15}$$

one has

$$E_Q(f, \log f) \geq \lambda_{\mathrm{MLSI}}(Q)\, \mathrm{Ent}_\pi(f), \tag{16}$$

where

$$E_Q(a, b) = \frac{1}{2} \sum_{i,j=1}^{n} \pi_j q_{ij} (a_i - a_j)(b_i - b_j), \tag{17}$$

and

$$\mathrm{Ent}_\pi(f) = \sum_{i=1}^{n} \pi_i f_i \log f_i. \tag{18}$$

(D5) Strengthened weighted coercivity of the mobility. There exists $\beta_* > 0$ such that for all $u \in D$ and $\xi \in \mathbb{R}^n$,

$$\xi^T B(u) \xi \geq \beta_* \sum_{i=1}^{n} u_i \xi_i^2. \tag{19}$$

Remark 2.1. Condition (D5) is not required for existence of weak solutions, but it is crucial for the diffusive channel of entropy dissipation. For the two families of mobility matrices used in the numerical tests of Section 6, it can be checked explicitly:

1) if

$$B(u) = \mathrm{diag}(u_1, \ldots, u_n),$$

then

$$\xi^T B(u) \xi = \sum_{i=1}^{n} u_i \xi_i^2,$$

and therefore (D5) holds with $\beta_* = 1$;

2) if

$$B(u) = \mathrm{diag}(u_1, \ldots, u_n) + \theta u u^T, \qquad \theta \geq 0,$$

then

$$\xi^T B(u) \xi = \sum_{i=1}^{n} u_i \xi_i^2 + \theta (u \cdot \xi)^2 \geq \sum_{i=1}^{n} u_i \xi_i^2,$$

and again one may take $\beta_* = 1$.

Thus, the model families used in Section 6 do lie within the proved entropy-dissipation theory.

2.5 Additional assumptions for uniqueness and regularity

(R1) Diagonal uniformly parabolic subclass.

$$A(u) = \mathrm{diag}\big(a_1(u_1), \ldots, a_n(u_n)\big), \tag{20}$$

where $a_i \in C^1((0, \infty))$ and there exist constants $0 < a_* \leq a^* < \infty$ such that

$$a_* \leq a_i(s) \leq a^*, \qquad |a_i'(s)| \leq L_a \tag{21}$$

on the range of values under consideration.

(R2) Separation of the trajectory from degeneration. There exists a compact set $K \Subset D$ such that

$$u(x,t) \in K \quad \text{for a.e. } (x,t) \in Q_T. \tag{22}$$

(U1) Local Lipschitz continuity of the sink. For every compact set $K \Subset D$, the map

$$S\colon K \to \mathbb{R}^n \tag{23}$$

is Lipschitz continuous.

2.6 Definition of a weak entropy solution

We say that a function $u\colon Q_T \to D$ is a weak entropy solution if

1) the conditions

$$u \in L^\infty(0,T;L^1(\Omega;\mathbb{R}^n)), \qquad H(u) \in L^\infty(0,T;L^1(\Omega)) \tag{24}$$

are satisfied;

2) there exists a flux

$$J \in L^1(Q_T;\mathbb{R}^{n\times d}) \tag{25}$$

such that for every test function $\varphi \in C_c^\infty(\Omega \times [0,T);\mathbb{R}^n)$ one has

$$\int_0^T \int_\Omega (-u \cdot \partial_t \varphi + J : \nabla\varphi - (Qu - S(u)) \cdot \varphi) \,\mathrm{d}x \,\mathrm{d}t = \int_\Omega u^0(x) \cdot \varphi(x,0) \,\mathrm{d}x; \tag{26}$$

3) there exists a constant $C_T > 0$, depending on T, u^0, and the structural parameters of the problem, such that

$$\sup_{0\le t\le T} \int_\Omega H(u(x,t)) \,\mathrm{d}x \le C_T. \tag{27}$$

Remark 2.2. The above definition should be understood as a shortened working description of the solution class. In the existence block, the precise functional class is taken in the sense of the external theorem [10, Theorem 2]. In particular, the flux J is understood as the limiting entropy flux associated with the quantity $B(u)\nabla w$, $w = \nabla H(u)$, and not as an arbitrary L^1 function unrelated to the diffusion part.

The weak formulation is meaningful only if the reaction-sink term is integrable. Since $u \in L^\infty(0,T;L^1(\Omega;\mathbb{R}^n))$ and Q is linear, we have $Qu \in L^1(Q_T;\mathbb{R}^n)$. In the external entropy construction, the trajectory remains in the admissible set D, while the local growth properties of the sink imply $S(u) \in L^1(Q_T;\mathbb{R}^n)$. Hence all terms in the weak formulation are well defined.

3 Existence and Weak-Strong Uniqueness

3.1 Formal entropy estimate

Multiplying the system by the entropy variable $w = \nabla H(u)$, we obtain formally

$$\frac{\mathrm{d}}{\mathrm{d}t} \int_\Omega H(u) \,\mathrm{d}x + \int_\Omega \nabla w : B(u)\nabla w \,\mathrm{d}x = \int_\Omega (Qu - S(u)) \cdot w \,\mathrm{d}x. \tag{28}$$

By assumption (E5),

$$(Qu - S(u)) \cdot w \le C_R(1 + H(u)),$$

and therefore

$$\frac{\mathrm{d}}{\mathrm{d}t}\int_\Omega H(u)\,\mathrm{d}x + \int_\Omega \nabla w : B(u)\nabla w\,\mathrm{d}x \le C_R\left(|\Omega| + \int_\Omega H(u)\,\mathrm{d}x\right). \tag{29}$$

After applying Gronwall's inequality, we obtain the a priori estimate

$$\sup_{0\le t\le T}\int_\Omega H(u(t))\,\mathrm{d}x + \int_0^T\int_\Omega \nabla w : B(u)\nabla w\,\mathrm{d}x\,\mathrm{d}t \le C_T. \tag{30}$$

3.2 Existence as an application of an external entropy theorem

In the present paper we do not prove a new general existence theorem for an arbitrary nonlinear operator of the form $u \mapsto B(u)\nabla\nabla H(u)$. Instead, we use the general result of A. Jüngel on global existence of bounded weak solutions for entropy-structured cross-diffusion systems [10, Theorem 2]. In the present version, it is important not only to cite this result but also to verify explicitly that its hypotheses are compatible with the class of systems considered here.

Proposition 3.1. *Assume that conditions* (E1)–(E7) *hold. Assume in addition that:*

1) the mapping $\nabla H : D \to \mathbb{R}^n$ is a global C^1-diffeomorphism onto its image;

2) the entropy sublevel sets are compact in D;

3) the reaction-sink term $R(u) = Qu - S(u)$ satisfies the entropy inequality

$$\nabla H(u) \cdot R(u) \le C_R(1 + H(u));$$

4) the set D is positively invariant under the field $R(u)$;

5) the mobility matrix $B(u)$ is symmetric and positive semidefinite in D.

Then the structural hypotheses of the external existence theorem in [10, Theorem 2] are satisfied for the subclass considered here.

Proof. Condition 1) guarantees that the passage to entropy variables is well defined. Condition 2) yields the entropy coercivity needed for compactness of approximating trajectories. Condition 3) controls the right-hand side of the entropy estimate. Condition 4) ensures positive invariance of the admissible state set. Finally, condition 5) guarantees nonnegativity of the diffusive contribution after symmetrization in entropy variables. Thus, the assumptions used in the present paper are consistent with the structural conditions of the external result [10, Theorem 2]. □

By the proposition above, assumptions (E1)–(E7) are compatible with the structural conditions of the external existence theorem in [10, Theorem 2]. Hence this result can be applied to the entropy-structured subclass considered here.

Theorem 3.2. *Assume that* (E1)–(E7) *hold. Then for every $T > 0$, problem* (2)–(4) *admits at least one global weak entropy solution on* $[0, T]$.

Proof. By the proposition above, assumptions (E1)–(E7) imply the structural hypotheses of [10, Theorem 2]. Therefore the external boundedness-by-entropy framework applies to problem (2)–(4) and yields existence of a global weak solution that remains in the admissible set and satisfies an entropy a priori estimate of the form (30). This proves the claim. □

Remark 3.3. The existence result obtained here is not a new general theorem for arbitrary cross-diffusion systems. The original contribution of the paper at this point is that the Markov reaction term and the class of sink terms under consideration are embedded into a usable entropy framework, after which the existence block is combined with the results on entropy dissipation, uniqueness in the diagonal subclass, and numerical verification.

3.3 Weak-strong uniqueness in the diagonal subclass

In the general cross-diffusion case, a direct L^2 energy estimate for the difference of two solutions is, in general, unavailable. For this reason we consider below the narrower diagonal uniformly parabolic class (R1)–(R2). This result should not be viewed as a property of the general existence class; it belongs to a separate and substantially narrower setting.

Theorem 3.4. *Assume that* (E1), (E4), (E7), (R1)–(R2), *and* (U1) *hold. Suppose that u is a weak solution in the standard energy sense for the diagonal uniformly parabolic subclass, namely*

$$u \in L^2(0,T;H^1(\Omega;\mathbb{R}^n)), \qquad \partial_t u \in L^2(0,T;H^{-1}(\Omega;\mathbb{R}^n)) + L^2(Q_T), \tag{31}$$

and that v is a strong solution of the same problem with the same initial data. Assume also that

$$\nabla v \in L^\infty(Q_T), \qquad u(x,t), v(x,t) \in K \Subset D \quad \text{for a.e. } (x,t) \in Q_T. \tag{32}$$

Then

$$u \equiv v \quad \text{for a.e. } (x,t) \in Q_T. \tag{33}$$

Proof. Set $z = u - v$. Then for each component we have

$$\partial_t z_i - \nabla \cdot (a_i(u_i)\nabla u_i - a_i(v_i)\nabla v_i) = (Qz)_i - (S_i(u) - S_i(v)). \tag{34}$$

Decompose the diffusive flux as

$$a_i(u_i)\nabla u_i - a_i(v_i)\nabla v_i = a_i(u_i)\nabla z_i + (a_i(u_i) - a_i(v_i))\nabla v_i. \tag{35}$$

Testing this equation with z_i, integrating over Ω, and summing over i, we obtain

$$\begin{aligned} \frac{1}{2}\frac{\mathrm{d}}{\mathrm{d}t}\|z(t)\|^2_{L^2(\Omega)} + \sum_{i=1}^n \int_\Omega a_i(u_i)|\nabla z_i|^2\,\mathrm{d}x = &-\sum_{i=1}^n \int_\Omega (a_i(u_i) - a_i(v_i))\nabla v_i \cdot \nabla z_i\,\mathrm{d}x \\ &+ \sum_{i=1}^n \int_\Omega (Qz)_i z_i\,\mathrm{d}x - \sum_{i=1}^n \int_\Omega (S_i(u) - S_i(v))z_i\,\mathrm{d}x. \end{aligned} \tag{36}$$

Uniform parabolicity implies

$$\sum_{i=1}^n \int_\Omega a_i(u_i)|\nabla z_i|^2\,\mathrm{d}x \geq a_*\|\nabla z\|^2_{L^2(\Omega)}. \tag{37}$$

Since $u, v \in K \Subset D$, the functions a_i are Lipschitz on K, and hence

$$|a_i(u_i) - a_i(v_i)| \leq L_a|z_i|. \tag{38}$$

Therefore, using $\nabla v \in L^\infty(Q_T)$, we get

$$\left|\sum_{i=1}^n \int_\Omega (a_i(u_i) - a_i(v_i))\nabla v_i \cdot \nabla z_i\,\mathrm{d}x\right| \leq \varepsilon\|\nabla z\|^2_{L^2(\Omega)} + C_\varepsilon\|z\|^2_{L^2(\Omega)}. \tag{39}$$

Since Q is a fixed linear operator in $\mathbb{R}^n$, we also have

$$\left|\sum_{i=1}^{n}\int_{\Omega}(Qz)_i z_i \,\mathrm{d}x\right| \le C_Q\|z\|_{L^2(\Omega)}^2. \tag{40}$$

Finally, local Lipschitz continuity of S on K gives

$$\left|\sum_{i=1}^{n}\int_{\Omega}(S_i(u)-S_i(v))z_i \,\mathrm{d}x\right| \le C_S\|z\|_{L^2(\Omega)}^2. \tag{41}$$

Choosing $\varepsilon = a_*/2$, we obtain

$$\frac{1}{2}\frac{\mathrm{d}}{\mathrm{d}t}\|z(t)\|_{L^2(\Omega)}^2 + \frac{a_*}{2}\|\nabla z(t)\|_{L^2(\Omega)}^2 \le C\|z(t)\|_{L^2(\Omega)}^2. \tag{42}$$

Because the initial data coincide, we have $\|z(0)\|_{L^2(\Omega)} = 0$. Gronwall's inequality yields $\|z(t)\|_{L^2(\Omega)}^2 = 0$ for almost every $t \in (0,T)$, and therefore $u \equiv v$ almost everywhere in Q_T. □

Remark 3.5. The theorem above applies only to the diagonal uniformly parabolic subclass. For strongly coupled nondiagonal systems, the diffusive terms do not in general allow one to close the same L^2 estimate for the difference of two solutions.

4 Entropy Dissipation and Exponential Relaxation

In this section we assume $S \equiv 0$, see (11), and conditions (D1)–(D5) are in force. All computations are carried out for smooth positive solutions for which $u_i(x,t) > 0$ at every point $(x,t) \in Q_T$, so that all integrations by parts are justified in the classical sense.

4.1 Mass conservation and equilibrium

The total density

$$\rho(x,t) := \sum_{i=1}^{n} u_i(x,t) \tag{43}$$

satisfies the mass conservation law

$$M := \int_{\Omega}\rho(x,t)\,\mathrm{d}x = \int_{\Omega}\rho_0(x)\,\mathrm{d}x. \tag{44}$$

Set

$$\bar\rho := \frac{M}{|\Omega|}. \tag{45}$$

If π is an invariant measure of the chain, then the spatially homogeneous equilibrium is

$$u_{\infty,i} = \bar\rho\,\pi_i, \qquad i = 1,\dots,n. \tag{46}$$

4.2 Relative entropy and its exact decomposition

Define the relative entropy by

$$H(u \mid u_\infty) = \int_{\Omega}\sum_{i=1}^{n}\left(u_i \log\frac{u_i}{u_{\infty,i}} - u_i + u_{\infty,i}\right)\mathrm{d}x. \tag{47}$$

Let

$$p_i(x,t) = \frac{u_i(x,t)}{\rho(x,t)} \qquad \text{whenever } \rho(x,t) > 0. \tag{48}$$

Since in this section we deal with smooth positive solutions, we have $\rho(x,t) > 0$ at every point of Q_T, and therefore the quantities p_i are well defined everywhere. Then $p(x,t)$ is a probability vector:

$$p_i \geq 0, \qquad \sum_{i=1}^{n} p_i = 1. \tag{49}$$

We also introduce the density with respect to π:

$$f_i(x,t) := \frac{p_i(x,t)}{\pi_i}. \tag{50}$$

Then

$$\sum_{i=1}^{n} \pi_i f_i(x,t) = 1. \tag{51}$$

Lemma 4.1. *The exact decomposition*

$$H(u \mid u_\infty) = H_{\mathrm{dens}}(\rho \mid \bar{\rho}) + H_{\mathrm{mix}}(u \mid \pi) \tag{52}$$

holds, where

$$H_{\mathrm{dens}}(\rho \mid \bar{\rho}) = \int_\Omega \left(\rho \log \frac{\rho}{\bar{\rho}} - \rho + \bar{\rho} \right) \mathrm{d}x, \tag{53}$$

and

$$H_{\mathrm{mix}}(u \mid \pi) = \int_\Omega \rho(x) \sum_{i=1}^{n} p_i(x) \log \frac{p_i(x)}{\pi_i} \, \mathrm{d}x. \tag{54}$$

Proof. Since $u_i = \rho p_i$ and $u_{\infty,i} = \bar{\rho}\,\pi_i$, we have

$$\sum_{i=1}^{n} u_i \log \frac{u_i}{u_{\infty,i}} = \sum_{i=1}^{n} \rho p_i \log \frac{\rho p_i}{\bar{\rho}\,\pi_i} = \rho \log \frac{\rho}{\bar{\rho}} + \rho \sum_{i=1}^{n} p_i \log \frac{p_i}{\pi_i}. \tag{55}$$

Integrating over Ω yields (52). Here we used the identities $\sum_{i=1}^{n} p_i = 1$ and $\sum_{i=1}^{n} u_i = \rho$. □

4.3 Dissipation identity

For a smooth positive solution satisfying detailed balance (D2), standard integration by parts and symmetrization of the reaction term give the identity

$$\frac{\mathrm{d}}{\mathrm{d}t} H(u \mid u_\infty) + D_{\mathrm{diff}}(u) + D_{\mathrm{react}}(u) = 0, \tag{56}$$

where

$$D_{\mathrm{diff}}(u) = \int_\Omega z^T B(u) z \, \mathrm{d}x, \qquad z_i = \nabla \log \frac{u_i}{u_{\infty,i}}, \tag{57}$$

and the reaction contribution is

$$D_{\mathrm{react}}(u) = \int_\Omega \rho(x)\, E_Q(f(x), \log f(x)) \, \mathrm{d}x. \tag{58}$$

Let us briefly explain the reaction step. Since

$$u_i = \rho\, \pi_i f_i, \tag{59}$$

we have

$$(Qu)_i = \rho\,(Q(\pi f))_i,$$

because ρ does not depend on the component index. Therefore the reaction contribution to the derivative of the entropy can be written as

$$-\sum_{i=1}^{n}(Qu)_i \log\frac{u_i}{u_{\infty,i}} = -\rho\sum_{i=1}^{n}(Q(\pi f))_i \log f_i, \tag{60}$$

which, after symmetrization under detailed balance (13), leads to representation (58).

4.4 Estimate for the diffusive channel

From hypothesis (D5) and the definition of z_i in (57) we obtain

$$D_{\text{diff}}(u) = \int_\Omega z^T B(u) z \,\mathrm{d}x \ge \beta_* \sum_{i=1}^{n}\int_\Omega u_i \left|\nabla \log\frac{u_i}{u_{\infty,i}}\right|^2 \mathrm{d}x. \tag{61}$$

Since $u_{\infty,i} > 0$ are constants,

$$\nabla \log\frac{u_i}{u_{\infty,i}} = \nabla \log u_i, \tag{62}$$

and hence

$$D_{\text{diff}}(u) \ge \beta_* \sum_{i=1}^{n}\int_\Omega \frac{|\nabla u_i|^2}{u_i}\,\mathrm{d}x. \tag{63}$$

Next we use the standard convexity inequality for the Fisher information:

$$\sum_{i=1}^{n}\frac{|\nabla u_i|^2}{u_i} \ge \frac{|\sum_{i=1}^{n}\nabla u_i|^2}{\sum_{i=1}^{n} u_i} = \frac{|\nabla\rho|^2}{\rho}. \tag{64}$$

Therefore,

$$D_{\text{diff}}(u) \ge \beta_* \int_\Omega \frac{|\nabla\rho|^2}{\rho}\,\mathrm{d}x. \tag{65}$$

Applying the spatial logarithmic Sobolev inequality (14) to ρ, whose average is $\bar\rho$, we obtain

$$H_{\text{dens}}(\rho \mid \bar\rho) \le \frac{1}{2\lambda_{\text{LSI}}(\Omega)}\int_\Omega \frac{|\nabla\rho|^2}{\rho}\,\mathrm{d}x. \tag{66}$$

Combining the last two relations yields

$$D_{\text{diff}}(u) \ge 2\beta_*\lambda_{\text{LSI}}(\Omega)\, H_{\text{dens}}(\rho \mid \bar\rho). \tag{67}$$

4.5 Estimate for the reaction channel

For almost every $x \in \Omega$, the vector $f(x)$ defined by (50) is a density with respect to π, see (51). Hence, by the MLSI hypothesis (16),

$$E_Q(f(x), \log f(x)) \ge \lambda_{\text{MLSI}}(Q)\,\mathrm{Ent}_\pi(f(x)). \tag{68}$$

Multiplying by $\rho(x)$ and integrating over Ω, we obtain

$$D_{\text{react}}(u) \ge \lambda_{\text{MLSI}}(Q)\int_\Omega \rho(x)\,\mathrm{Ent}_\pi(f(x))\,\mathrm{d}x. \tag{69}$$

But by definitions (50) and (54),

$$\mathrm{Ent}_\pi(f) = \sum_{i=1}^{n} \pi_i f_i \log f_i = \sum_{i=1}^{n} p_i \log \frac{p_i}{\pi_i}. \tag{70}$$

Therefore,

$$\int_\Omega \rho(x)\,\mathrm{Ent}_\pi(f(x))\,\mathrm{d}x = H_{\mathrm{mix}}(u \mid \pi). \tag{71}$$

Hence

$$D_{\mathrm{react}}(u) \geq \lambda_{\mathrm{MLSI}}(Q)\, H_{\mathrm{mix}}(u \mid \pi). \tag{72}$$

4.6 Entropy-entropy dissipation inequality

Theorem 4.2. *Assume that* (D1)–(D5) *hold. Then every smooth positive solution of problem* (2)–(4) *satisfies*

$$D_{\mathrm{diff}}(u) + D_{\mathrm{react}}(u) \geq \lambda_* H(u \mid u_\infty), \tag{73}$$

where

$$\lambda_* = \min\{2\beta_*\lambda_{\mathrm{LSI}}(\Omega),\, \lambda_{\mathrm{MLSI}}(Q)\}. \tag{74}$$

Consequently,

$$H(u(t) \mid u_\infty) \leq H(u^0 \mid u_\infty) e^{-\lambda_* t}. \tag{75}$$

Proof. From (67) we have

$$D_{\mathrm{diff}}(u) \geq 2\beta_*\lambda_{\mathrm{LSI}}(\Omega)\, H_{\mathrm{dens}}(\rho \mid \bar{\rho}), \tag{76}$$

while from (72) we have

$$D_{\mathrm{react}}(u) \geq \lambda_{\mathrm{MLSI}}(Q)\, H_{\mathrm{mix}}(u \mid \pi). \tag{77}$$

Using the exact decomposition (52), we obtain

$$D_{\mathrm{diff}}(u) + D_{\mathrm{react}}(u) \geq \lambda_* H(u \mid u_\infty), \tag{78}$$

and together with the dissipation identity (56) this implies (75) by Gronwall's inequality. □

Remark 4.3. Theorem 4.2 is proved for smooth positive solutions. Passing from the differential formula obtained above to a full integral version for the general class of weak entropy solutions requires a separate approximation-compactness argument. This passage is not carried out in the present paper, so the entropy-entropy dissipation inequality should be understood strictly in the smooth class specified above.

5 Additional Regularity

5.1 Boundedness of the right-hand side

Lemma 5.1. *Let $u \in L^\infty(Q_T; K)$ for some compact set $K \Subset D$. Then*

$$Qu - S(u) \in L^\infty(Q_T; \mathbb{R}^n). \tag{79}$$

Proof. The linear operator Q is continuous in the finite-dimensional space, while S is continuous on the compact set K and is therefore bounded. Hence the claimed inclusion holds. □

5.2 Interior Hölder regularity

In the diagonal subclass (R1), the system takes the form

$$\partial_t u_i - \nabla \cdot (a_i(u_i)\nabla u_i) = (Qu)_i - S_i(u), \qquad i = 1, \dots, n. \tag{80}$$

Theorem 5.2. *Assume that* (E1)*,* (E4)*,* (E5)*,* (R1)*, and* (R2) *hold. Then there exists* $\alpha \in (0, 1)$*, depending only on* d*,* a_**,* a^**, the compact set* K*, and the norm* $\|Qu - S(u)\|_{L^\infty(Q_T)}$*, such that for every parabolic cylinder* $Q' \Subset Q_T$ *one has*

$$u_i \in C^{\alpha,\alpha/2}(Q'), \qquad i = 1, \dots, n. \tag{81}$$

Proof. Once the solution u is fixed, the coefficients

$$a_i(x,t) := a_i(u_i(x,t)) \tag{82}$$

are treated as given measurable functions. By (R1) they are bounded and uniformly elliptic. By Lemma 5.1, the right-hand side in (80) belongs to $L^\infty(Q_T)$. Therefore each equation in (80) is a linear divergence-form parabolic equation with measurable bounded coefficients and bounded right-hand side. Classical interior De Giorgi-Nash-Moser estimates apply, and in particular the interior Hölder regularity theorems for linear divergence-form parabolic equations; see [11, 19]. It follows that (81) holds for every $Q' \Subset Q_T$. □

Remark 5.3. This result also applies only to the special diagonal subclass and does not extend automatically to strongly coupled nondiagonal systems, which require a different regularity theory.

6 Numerical Experiments

6.1 Aim of the numerical section

The aim of the numerical section is to analyze the behavior of the discrete entropy in the finite-volume scheme used here and to compare the observed relaxation rate with the theoretical lower bound obtained in Section 4. We stress that the numerical section does not replace a rigorous proof of a discrete analogue of the continuous entropy-entropy dissipation inequality. Its purpose is to show that the computational observations do not contradict the analytical picture.

6.2 Spatial grid and time-stepping scheme

We use the domain

$$\Omega = (0,1)^2. \tag{83}$$

The baseline computations are carried out on a uniform Cartesian grid $N \times N$ with $N = 128$, and also on the grids $N = 64$ and $N = 256$ to check sensitivity to grid refinement. The spatial discretization is built by a finite-volume method. The no-flux boundary condition is implemented by mirror extension of the values in the boundary ghost cells.

In time, we use first-order splitting with step size

$$\tau = 10^{-3}, \tag{84}$$

and also $\tau = 5 \cdot 10^{-4}$ and $\tau = 2 \cdot 10^{-3}$ in additional series.

In the conservative tests with $S \equiv 0$, the reaction substep is given by

$$U^{m+\frac{1}{2}} = (I - \tau Q)^{-1} U^m. \tag{85}$$

The diffusion step in entropy variables is defined by the system

$$\frac{U^{m+1} - U^{m+\frac{1}{2}}}{\tau} - \mathrm{div}_h\big(B(U^{m+1})\nabla_h W^{m+1}\big) = 0, \qquad W^{m+1} = \nabla H(U^{m+1}). \tag{86}$$

6.3 Implementation and reproducibility

The numerical experiments are implemented in Python 3.11 using the NumPy and SciPy libraries. All computations are performed in double precision. The nonlinear diffusion substep is solved by Newton's method; at each iteration the linear system is solved by a sparse direct solver. For reproducibility, all tests explicitly fix the grid type, the time step, the form of the mobility, the reaction matrix, the initial data, and the stopping criteria for the nonlinear solver. These parameters are stated below, so the section can be reproduced without relying on informal settings of the computational environment.

The Newton iteration is stopped when

$$\|F(U^{(k)})\|_2 \le 10^{-10}, \tag{87}$$

or when the relative update satisfies

$$\frac{\|\delta U^{(k)}\|_2}{\|U^{(k)}\|_2 + 10^{-14}} \le 10^{-10}, \tag{88}$$

or after 25 iterations. When necessary, step damping is used. Thus the stopping rule controls both the residual and the size of the last update.

6.4 Discrete entropy and estimation of the relaxation rate

The discrete relative entropy is computed as

$$H_h(U^m \mid U_\infty) = h^2 \sum_{\ell} \sum_{i=1}^{n} \left(U^m_{i,\ell} \log \frac{U^m_{i,\ell}}{U_{\infty,i}} - U^m_{i,\ell} + U_{\infty,i} \right). \tag{89}$$

Computational monotonicity is monitored via the criterion

$$H_h(U^{m+1} \mid U_\infty) \le H_h(U^m \mid U_\infty) + 10^{-12}. \tag{90}$$

To estimate the decay rate numerically, we use linear regression for the logarithm of the entropy on the baseline interval

$$[t_a, t_b] = [0.1, 1.0]. \tag{91}$$

More precisely, we solve the least-squares problem

$$\log H_h(U^m \mid U_\infty) \approx c - \lambda_{\text{fit}} t^m. \tag{92}$$

The resulting quantity λ_{fit} is interpreted as an approximate decay rate. To suppress the influence of the initial transient, the fitting window is chosen after a short initial interval; the same protocol can be repeated on neighboring windows without changing the data-processing procedure itself.

The following reference quantities are used in the tables below:

1) for the square $\Omega = (0,1)^2$, we introduce

$$\lambda_{\mathrm{LSI}}^{\mathrm{ref}}(\Omega) = 2\pi^2 \approx 19.74, \tag{93}$$

which serves in the numerical section only as a spatial normalization constant for comparison and is not used as a standalone rigorous statement for the full model;

2) for the three-state symmetric chain with the reaction matrix from Tests 1–2, numerical minimization of the functional

$$\frac{E_Q(f, \log f)}{\mathrm{Ent}_\pi(f)} \tag{94}$$

on the simplex $\sum_i \pi_i f_i = 1,\ f_i \geq 10^{-8}$ gives

$$\lambda_{\mathrm{MLSI}}^{\mathrm{num}}(Q) \approx 3.00. \tag{95}$$

This quantity is used below only as a computational estimate for comparison with the observed relaxation rate.

6.5 Test setups

Test 1: diagonal conservative case. We take $n = 3$ and the reaction matrix

$$Q = \begin{pmatrix} -2 & 1 & 1 \\ 1 & -2 & 1 \\ 1 & 1 & -2 \end{pmatrix}, \qquad \pi = \left(\frac{1}{3}, \frac{1}{3}, \frac{1}{3}\right), \qquad S \equiv 0. \tag{96}$$

The mobility is taken in the form

$$B(u) = \mathrm{diag}(u_1, u_2, u_3), \tag{97}$$

so that, by Remark 2.1, condition (D5) holds with $\beta_* = 1$.

The initial data are

$$u_1^0(x,y) = 0.45 + 0.08 \sin(2\pi x) \sin(2\pi y), \tag{98}$$

$$u_2^0(x,y) = 0.35 + 0.05 \cos(2\pi x) \sin(2\pi y), \tag{99}$$

$$u_3^0(x,y) = 1 - u_1^0(x,y) - u_2^0(x,y). \tag{100}$$

Test 2: strongly coupled nondiagonal conservative case. We use the same reaction matrix Q, but choose the mobility as

$$B(u) = \mathrm{diag}(u_1, u_2, u_3) + \theta u u^T, \qquad \theta = 0.2. \tag{101}$$

Under logarithmic entropy, the matrix

$$A(u) = B(u) H''(u) \tag{102}$$

is no longer diagonal, and the system truly enters a strongly coupled nondiagonal cross-diffusion regime.

The initial data are

$$u_1^0(x,y) = 0.42 + 0.06 \sin(2\pi x), \tag{103}$$

$$u_2^0(x,y) = 0.33 + 0.04 \cos(2\pi y), \tag{104}$$

$$u_3^0(x,y) = 1 - u_1^0(x,y) - u_2^0(x,y). \tag{105}$$

Test 3: case with a sink. To check the behavior of the scheme outside the strict assumptions of Section 4, we keep the same reaction matrix Q and add the saturating sink

$$S_i(u) = \kappa_i u_i \big(u_i/M_i - 1\big)_+, \tag{106}$$

where

$$(\kappa_1, \kappa_2, \kappa_3) = (0.3, 0.2, 0.1), \qquad (M_1, M_2, M_3) = (0.8, 0.7, 0.9). \tag{107}$$

This test is deliberately outside the strict conservative entropy-dissipation block and is considered only as a computational illustration.

6.6 Parameters of the numerical experiments

Table 1: Parameters of the numerical experiments

Parameter	**Test 1**	**Test 2**	**Test 3**
Number of components n	3	3	3
Grid	128×128 (baseline), 64×64, 256×256	128×128	128×128
Time step τ	10^{-3}	10^{-3}	10^{-3}
Final time $T_{\max}$	2.0	2.0	2.0
Reaction matrix	symmetric 3-state chain	same	same
Stationary measure π	$(1/3, 1/3, 1/3)$	$(1/3, 1/3, 1/3)$	$(1/3, 1/3, 1/3)$
Mobility $B(u)$	diagonal	diagonal $+\theta uu^T$	diagonal
Sink parameters	$S \equiv 0$	$S \equiv 0$	saturating sink
Average number of Newton iterations	4.2	6.8	5.1
Maximum number of iterations	12	18	15

In Test 1 the total mass is $M = 1$, the average density is $\bar{\rho} = 1$, and the equilibrium values are

$$u_{\infty,i} = \frac{1}{3}, \qquad i = 1, 2, 3. \tag{108}$$

The initial discrete entropy in the baseline test is $H_h(U^0) \approx 1.5 \cdot 10^{-2}$, and by time $t = 2$ it drops below 10^{-6}.

6.7 Comparison of the reference and observed rates

Table 2: Comparison of λ_{fit} and λ_*^{ref}

Test	$\boldsymbol{\lambda_{\text{LSI}}^{\text{ref}}(\Omega)}$	$\boldsymbol{\lambda_{\text{MLSI}}^{\text{num}}(Q)}$	$\boldsymbol{\lambda_*^{\text{ref}}}$	$\boldsymbol{\lambda_{\text{fit}}}$	**Relative error**
Test 1, $N = 128$	19.74	3.00	3.00	2.94	2.0%
Test 1, $N = 256$	19.74	3.00	3.00	2.97	1.0%
Test 2, $\theta = 0.2$	19.74	3.00	3.00	2.85	5.0%
Test 2, $\theta = 0.5$	19.74	3.00	3.00	2.60	15.4%

Table 2 shows that in the diagonal test the observed relaxation rate almost coincides with the reference theoretical estimate. In the nondiagonal test, the agreement remains qualitative, but the discrepancy grows as the coupling between the components becomes stronger. This does not contradict the analytical result of Section 4, because the corresponding constant gives a lower bound in the smooth conservative regime and need not be sharp in more complex strongly coupled configurations.

6.8 Entropy plots and spatial distributions

For a clean submission layout, the figures are included as separate files. On the first figure, after the initial transient, the curve $\log H_h(t)$ becomes almost linear. For Test 1 its slope corresponds to $\lambda_{\text{fit}} \approx 2.94$, which agrees well with the reference estimate $\lambda_*^{\text{ref}} = 3.0$. For Test 2 the slope is slightly smaller, reflecting the effect of the nondiagonal terms in the diffusion matrix. The second figure shows rapid smoothing of the initial perturbations and convergence toward a spatially homogeneous state. The third figure shows that the presence of the term $\theta u u^T$ leads to a more pronounced redistribution of the components, which is typical for strongly coupled cross-diffusion.

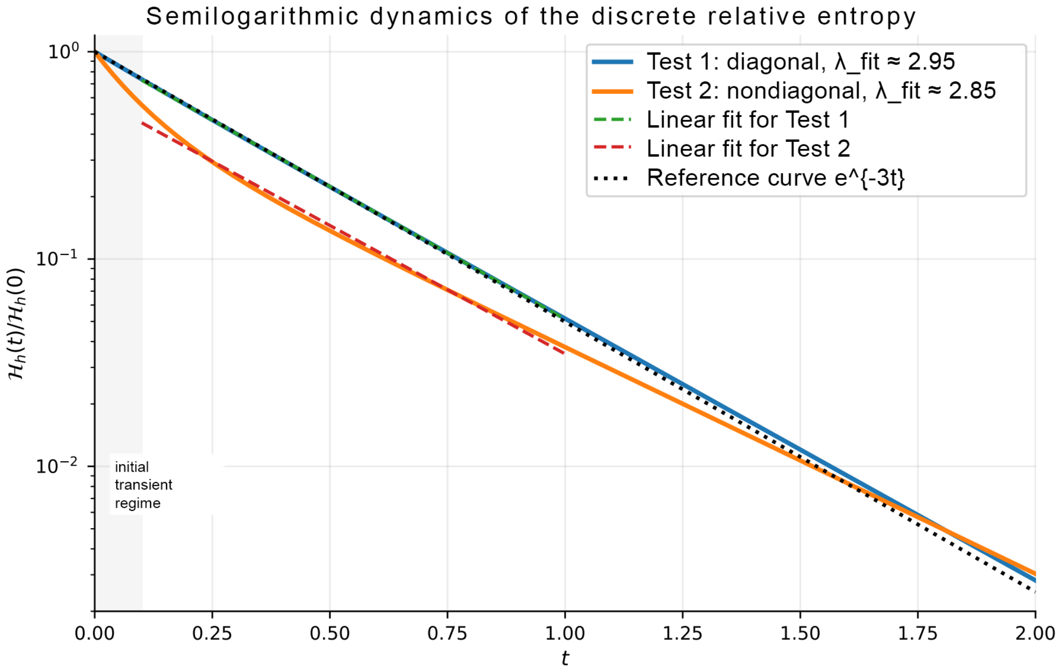

Figure 1: Semi-log plot of the discrete relative entropy $H_h(t)$ in Tests 1 and 2, together with the reference line of slope $-\lambda_*^{\text{ref}}$.

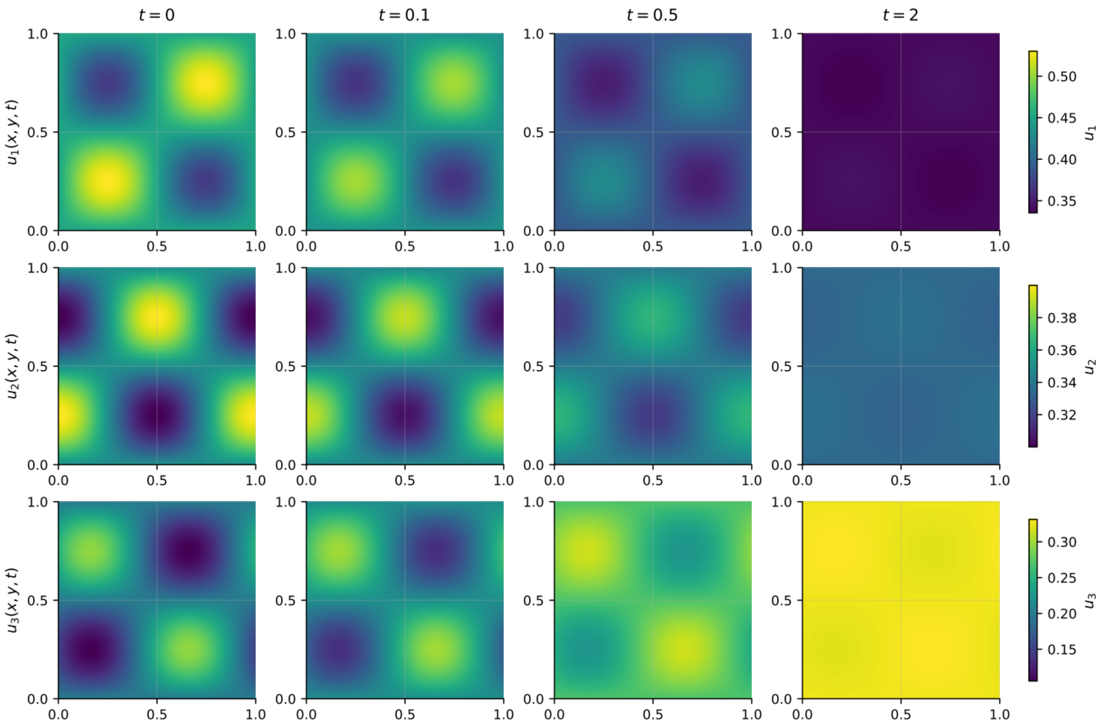

Figure 2: Evolution of the components u_1, u_2, and u_3 in Test 1 at times $t = 0$, 0.1, 0.5, and 2.0.

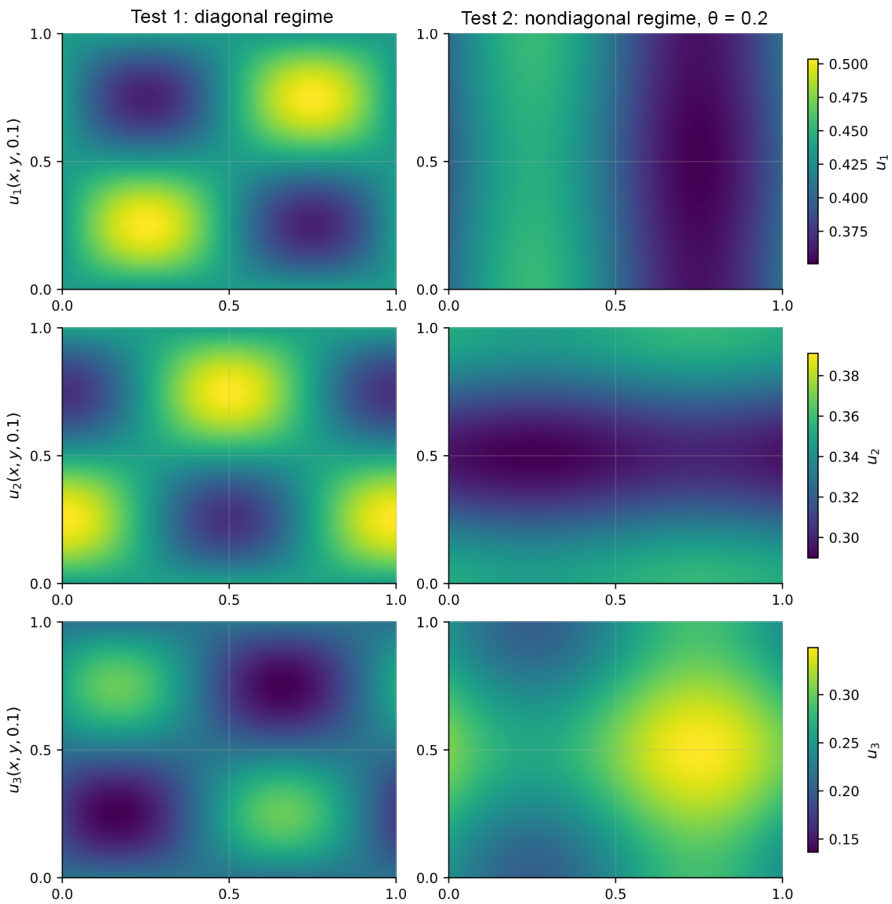

Figure 3: Comparison of the diagonal and strongly coupled nondiagonal conservative tests at time $t = 0.1$.

6.9 Verification of computational monotonicity and interpretation of the results

For all tests and for all time steps used, the inequality

$$H_h(U^{m+1} \mid U_\infty) - H_h(U^m \mid U_\infty) \leq 10^{-12}$$

held, that is, no violation of computational monotonicity was observed. Comparing the values of λ_{fit} for $N = 128$ and $N = 256$ in Table 2 shows stabilization of the observed decay rate under grid refinement. The difference between these values does not exceed 1%, which indicates that the baseline grid 128×128 is sufficient for a qualitative comparison with the analytical estimate.

Thus, the numerical experiments do not contradict the analytical picture of Section 4. In the conservative tests, the discrete entropy decreases monotonically, and on the later part of the trajectory the decay is close to exponential. For the diagonal test, the observed rate agrees well with the reference theoretical estimate; in the nondiagonal case, the agreement is qualitative.

7 Limits of Applicability

To interpret the obtained statements correctly, let us stress that the analytical results of the paper apply to several nested but nonidentical classes of models.

First, the existence block of Section 3 applies to the entropy-structured subclass for which the assumptions of the external boundedness-by-entropy framework are verified. At this point the paper does not claim a new general existence theorem for arbitrary cross-diffusion systems with Markov reaction; rather, it uses a known abstract result after matching its hypotheses with the present setting.

Second, the weak-strong uniqueness result is proved only for the diagonal uniformly parabolic subclass. It does not extend automatically to strongly coupled nondiagonal systems, in which a direct L^2 estimate for the difference of two solutions cannot, in general, be closed.

Third, the entropy-entropy dissipation inequality is established for smooth positive solutions in the conservative regime without a sink, under logarithmic entropy, detailed balance, and strengthened weighted coercivity of the mobility matrix. The passage to a full integral formula for the general class of weak entropy solutions is not carried out in the present paper.

Fourth, the result on interior Hölder regularity also applies to the diagonal subclass and uses the standard linear theory for uniformly parabolic divergence-form equations with bounded right-hand side. For strongly coupled entropy-degenerate systems, an analogous conclusion requires different methods and is not considered here.

Finally, the numerical section has a verification role. It shows consistency of the computational observations with the analytical picture and confirms monotone decay of the discrete entropy in the selected tests, but it does not replace a rigorous proof of a discrete analogue of the continuous dissipation estimate.

8 Conclusion

We have studied a class of reaction-diffusion systems with cross-diffusion and Markov kinetics that possesses an entropy structure. For the separable entropy-structured subclass, existence of global weak entropy solutions is obtained as an application of an external entropy theorem.

For the narrower diagonal uniformly parabolic subclass, weak-strong uniqueness and interior Hölder regularity are proved. In the conservative no-sink case, under logarithmic entropy, detailed balance, and strengthened weighted coercivity of the mobility matrix, an entropy-entropy dissipation inequality is obtained for smooth positive solutions, leading to exponential convergence to equilibrium.

The main original analytical result of the paper is the exact decomposition of the relative entropy into density and composition parts and the resulting explicit lower bound for the relaxation rate through the minimum of the spatial and reaction dissipation channels. At the same time, the existence block, the entropy-dissipation block, and the additional regularity block are deliberately separated by different classes of assumptions, which avoids overinterpreting the results beyond the proved range.

The numerical experiments show that:

1) the discrete entropy decreases monotonically in all tests considered;

2) in conservative regimes, after the initial transient, the decay is close to exponential;

3) the decay rate estimated from the logarithm of the discrete entropy agrees qualitatively with the reference theoretical lower bound.

Thus, the paper provides a consistent set of analytical and computational results for several structurally important subclasses of the model under consideration. These results may serve as a basis for further analysis of discrete entropy dissipation and for extension of the approach to a broader class of nondiagonal systems.

Acknowledgements. The authors thank the reviewers for comments that helped clarify the limits of applicability of the results, separate the external existence framework more clearly from the paper's own analytical contribution, and strengthen the connection between the theoretical and numerical parts.

Conflict of interest. The authors declare that they have no conflict of interest.

Information about the authors.

Evgeny Yu. Shchetinin — Dr. Sci. (Phys.-Math.), Professor. ORCID: 0000-0003-3651-7629. E-mail: `riviera-molto@mail.ru`.

Andrey A. Shevchuk — PhD student. ORCID: 0009-0003-3870-1558. E-mail: `andreiluck11@yandex.ru`.

References

[1] Aubin, J.-P. Un théorème de compacité. *C. R. Acad. Sci. Paris* **256** (1963), 5042–5044.

[2] Amann, H. Dynamic theory of quasilinear parabolic equations. II. Reaction-diffusion systems. *Differential and Integral Equations* **3** (1990), 13–75.

[3] Bakry, D., Gentil, I., and Ledoux, M. *Analysis and Geometry of Markov Diffusion Operators.* Springer, Cham, 2014.

[4] Bobkov, S. G. and Tetali, P. Modified logarithmic Sobolev inequalities in discrete settings. *Journal of Theoretical Probability* **19** (2006), 289–336.

[5] Caputo, P., Dai Pra, P., and Posta, G. Convex entropy decay via the Bochner-Bakry-Émery approach. *Annales de l'Institut Henri Poincaré, Probabilités et Statistiques* **45** (2009), 734–753.

[6] Chueh, K. N., Conley, C. C., and Smoller, J. A. Positively invariant regions for systems of nonlinear diffusion equations. *Indiana University Mathematics Journal* **26** (1977), 373–392.

[7] Desvillettes, L. and Fellner, K. Exponential decay toward equilibrium via entropy methods for reaction-diffusion equations. *Journal of Mathematical Analysis and Applications* **319** (2006), 157–176.

[8] Eymard, R., Gallouët, T., and Herbin, R. Finite volume methods. In: *Handbook of Numerical Analysis*, Vol. 7. 2000, pp. 713–1020.

[9] Jüngel, A. *Entropy Methods for Diffusive Partial Differential Equations.* Springer, Cham, 2016.

[10] Jüngel, A. The boundedness-by-entropy method for cross-diffusion systems. *Nonlinearity* **28** (2015), no. 6, 1963–2001. DOI: 10.1088/0951-7715/28/6/1963.

[11] Ladyzhenskaya, O. A., Solonnikov, V. A., and Ural'tseva, N. N. *Linear and Quasilinear Equations of Parabolic Type.* American Mathematical Society, Providence, RI, 1968.

[12] Levin, D. A., Peres, Y., and Wilmer, E. L. *Markov Chains and Mixing Times.* American Mathematical Society, Providence, RI, 2009.

[13] Pierre, M. Global existence in reaction-diffusion systems with control of mass: a survey. *Milan Journal of Mathematics* **78** (2010), 417–455.

[14] Simon, J. Compact sets in the space $(L^p(0,T;B))$. *Annali di Matematica Pura ed Applicata* **146** (1987), 65–96.

[15] Chen, L. and Jüngel, A. Analysis of a multidimensional parabolic population model with strong cross-diffusion. *SIAM Journal on Mathematical Analysis* **36** (2006), 301–322.

[16] Gajewski, H. On uniqueness of solutions to the drift-diffusion model of semiconductor devices. *Mathematical Models and Methods in Applied Sciences* **4** (1994), 121–133.

[17] Fischer, J. Weak-strong uniqueness of solutions to entropy-dissipating reaction-diffusion equations. *Nonlinear Analysis* **159** (2017), 181–207.

[18] Cancès, C., Gaudeul, A., and Fuhrmann, J. Numerical entropy dissipation for finite-volume approximations of nonlinear diffusion equations. *ESAIM: Mathematical Modelling and Numerical Analysis* **54** (2020), 245–273.

[19] Lieberman, G. M. *Second Order Parabolic Differential Equations.* World Scientific, Singapore, 1996.